Journal of Radioanalytical and Nuclear Chemistry (2022) 331:3005–3014
https://doi.org/10.1007/s10967-022-08352-8

Sorption of uranium(VI) from aqueous solution using nanomagnetite particles; with and without humic acid coating

Aly A. Helal[1] · I. M. Ahmed[1,2] · R. Gamal[1] · S. A. Abo-El-Enein[3] · A. A. Helal[1]

Received: 3 February 2022 / Accepted: 28 April 2022 / Published online: 12 June 2022

Abstract
In this study, iron oxide nanoparticles (Fe_3O_4) and iron oxide nanoparticles with humic acid coatings (Fe_3O_4/HA) were investigated for the removal of U(VI). The effect of contact time, adsorbent mass, U(VI) concentration, and pH was studied by batch technique. The sorption kinetic data follows pseudo-second order, while the isotherms obey Langmuir with Q_{max} values of 238.0, 195.6 mg/g for Fe_3O_4 and Fe_3O_4/HA, respectively. According to the study, humic acid decreases the sorption capacity of magnetite due to the formation of a polyanionic organic coating, altering the surface properties of the particles, reducing magnetite aggregation, and stabilizing magnetite suspension.

Keywords Sorption · Nanomagnetite · Humic acid coated nanomagnetite · Uranium(VI)

Introduction

Nuclear activities produce hazardous wastes that are varying in their source, chemical composition, physical state, in addition to their radioactivity. The waste coming from the nuclear facilities is very toxic and carcinogenic as it contains U(VI) ions that implies good practice in radioactive waste management to protect living organisms and the environment from radiation.

The World Health Organization (WHO) has reported the maximum amount of uranium in drinking water as 0.2 ppm [1]. Numerous techniques were proposed to eliminate the uranium and its fission products from surface and groundwater, and waste streams as ion exchange, liquid–liquid extraction, precipitation and adsorption. Ion exchange and adsorption techniques are the most effective methods as they characterized by their simplicity and low operating costs [2, 3]. Many adsorbents as clay minerals, polymers and biomass showed low sorption capacities that limit their use [4].

✉ Aly A. Helal
alyhelal@hotmail.com

[1] Hot Laboratories and Waste Management Center, Egyptian Atomic Energy Authority, Cairo 13759, Egypt

[2] Chemistry Department, College of Science, Jouf University, Skaka, Saudi Arabia

[3] Faculty of Science, Ain Shams University, Cairo, Egypt

Recently, magnetic nanoparticles (MNP) have drawn attention due to their large surface area, little internal diffusion resistance, high stability, shape-controlled, high magnetism and high separation convenience and narrow size distribution. However, such adsorbents have some drawbacks as they are highly susceptible to air oxidation and liable to aggregation that reduces their sorption efficiency. To overcome these two drawbacks, various modifications have been introduced on MNP surfaces as coupling with organic polymer, organic surfactants, inorganic oxides, bioactive molecules and humic substances; [humic acid (HA), fulvic acids (FA), and humin] that exhibit strong complexation with metal ions and organic dyes [5–12]. The humic materials are thought to have a distinct role in the environmental mobility of metals. In natural water systems where humic acid is existent, the complexation with humic acid plays a major role in the geochemical behavior and migration of uranium and its fission products in the geosphere. Many of radioactive materials have variable degrees of sympathy for humic materials. They are capable of reacting with humic compounds producing organometal complexes of different stability and solubility. These organometal reactions control the final fate of the metallic ions in soils, sediments, and water. The presence of these substances enables the mobilization, segregation, transport, and deposition of trace metals in soil, sediments, biogenic deposits and sedimentary rocks of several types. They play a key role in the chemical weathering of rocks and minerals, and they function as carriers of metal ions in natural waters; a portion

of the trace metals found in soils and sediments, as well as coal and other biogenic deposits occurs in organically bound forms. Several authors have indicated the high affinity of humic substances for actinide and lanthanide metal ions, and their strong influence on the distribution of the metal ions. Illésand Tombácz [13] indicated that humic acid has high affinity to Fe_3O_4 nanoparticles and improves the constancy of nanodispersions by preventing their accumulation. Many authors investigated the use of magnetic nanoparticles in the extraction of uranium from water and sea water matrix [14–18]. The aim of this work is focused on the investigation of the sorption behavior of uranium ions onto magnetite nanoparticles (Fe_3O_4) and humic acid coated magnetite nanoparticles (Fe_3O_4/HA) as humic materials are the most prevalent in the environment, and it was necessary to take them into account.

Experimental

Reagents and instrumentation

Analytical grade of $FeCl_3$, $FeSO_4{\cdot}7H_2O$, NaOH, $UO_2(NO_3)_2{\cdot}6H_2O$ and "humic acid" were purchased from Merck and "Aldrich", and were used without any further purification. The microstructure of the Fe_3O_4 and Fe_3O_4/HA was investigated by FTIR spectrometer (a Nicolet spectrometer from Meslo, USA). Mineralogical analysis of the sample was determined by XRD using a Shimadzu-6000, Japan) diffractometer. The surface morphology of Fe_3O_4 and Fe_3O_4/HA is investigated by transmission electron microscope, TEM(Hitachi-H800, Japan). A pH meter of Hanna instruments type was used to monitor the hydrogen ion concentration for the solutions. In the sorption experiments, a good mixing of the two phases was achieved by using a thermostated shaker of the type Julapo (Germany). The concentration of uranium was estimated using Shimadzu UV/Vis, double beam recording spectrophotometer, Model 160-A, Japan.

Synthesis of magnetite nanoparticles and humic acid coated magnetite nanoparticles

The two investigated adsorbents were prepared by a co-precipitation method. Briefly, $FeCl_3$ and $FeSO_4.7H_2O$ were mixed with a molar ratio 2:1 at 80 °C, and then precipitated by1.0 M NaOH, drop by drop, with vigorous stirring under nitrogen atmosphere. The black precipitate was collected and washed several times with distilled water and dried. The humic acid coated nanomagnetite was synthesized by adding humic acid (0.5 g/L) dissolved in concentrated ammonia. The Fe^{3+} and Fe^{2+}(2:1) mixture was added, drop by drop, under nitrogen atmosphere until black precipitate is obtained, which is collected, washed and dried.

Batch adsorption procedure

In the batch experiments, 5.0 mg from both Fe_3O_4 and Fe_3O_4/HA were shaken with 20.0 mL from U(VI) ions with initial concentration of 50 mg/L for 2.0 h, at pH values of 7.0 and 5.5 respectively, and at 25 °C unless otherwise stated. The sorbents were separated by using a magnet, and the solution was centrifuged for U(VI) measurement by UV–Vis spectrophotometer using Arsenazo(III) method [19]. The percent uptake was calculated as follows:

$$\text{Uptake}\% = \left(C_\text{i} - C_\text{f}\right)/C_\text{i} * 100 \quad (1)$$

where C_i and C_f are the initial and final concentrations, respectively.

The amount of U(VI) sorbed by the nanoparticles, q_e (mg/g) was estimated using the following relation:

$$q_\text{e} = \left(C_\text{i} - C_\text{f}\right) * V/m \quad (2)$$

where V and m refer to the solution volume in L and the sorbent weight in g, respectively.

Results and discussion

Characterization of sorbents

Figure 1 shows the phase composition of the magnetite and humic acid coated nanoparticles which were analyzed by XRD. The Fe_3O_4 particles show peaks at 2θ values of 30.22, 35.6, 42.4, 58.4 and 62.78, which are characteristic for the magnetite spinel structure [20]. The diffraction of Fe_3O_4/HA shows the same reflection peaks of Fe_3O_4; indicating that the HA coating does not corrupt the core of magnetite nanoparticles. The chemical structure of adsorbent was

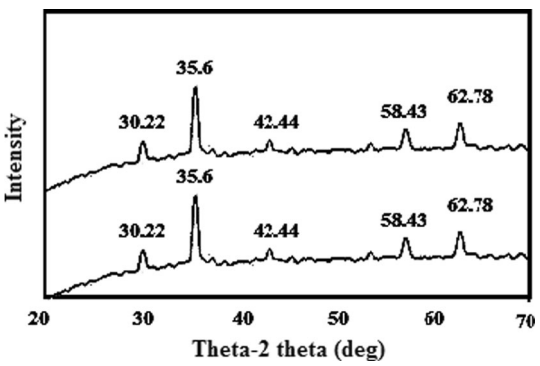

Fig. 1 XRD of Fe_3O_4 and Fe_3O_4/HA nanoparticles

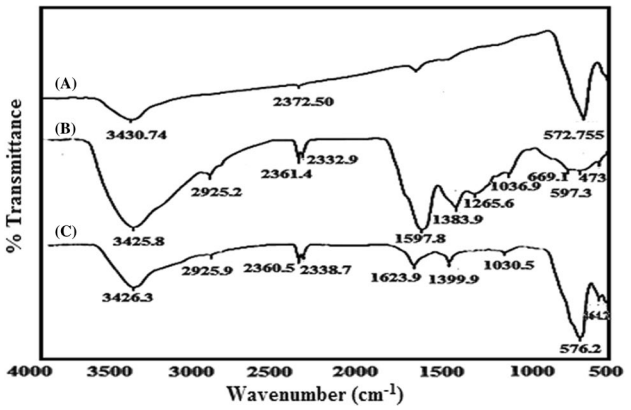

Fig. 2 IR spectra of **A** magnetite nanoparticles **B** Humic acid **C** humic acid coated magnetite nanoparticles

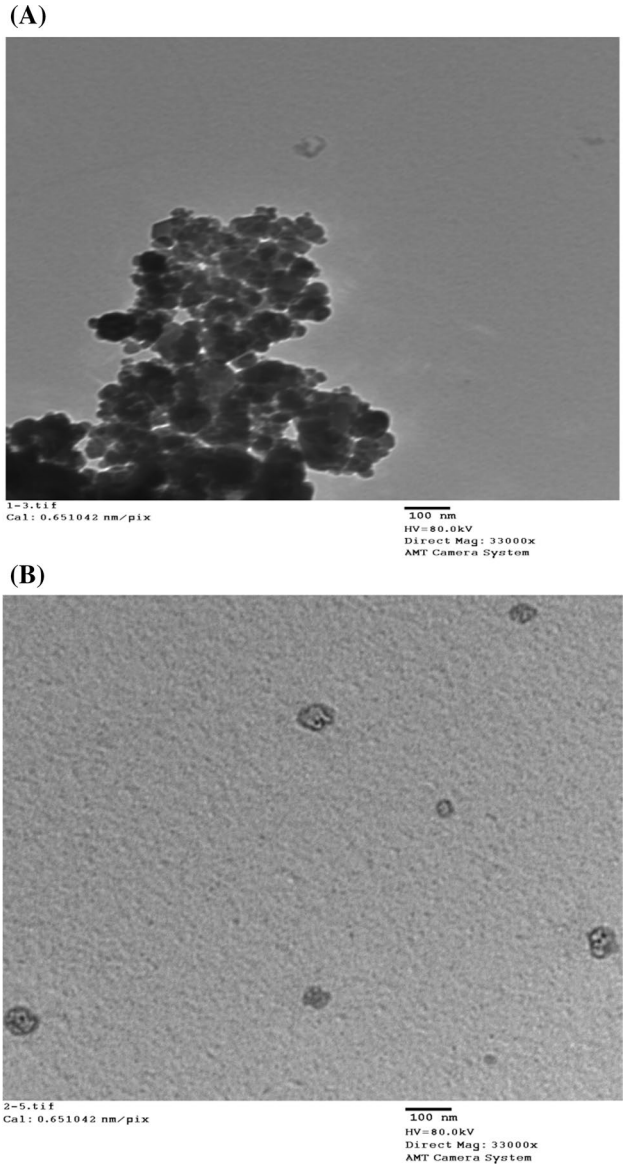

Fig. 3 **a** TEM image for Fe_3O_4 nanoparticles. **b** TEM image for Fe_3O_4/HA nanoparticles

determined by FTIR. Figure 2a, b shows a characteristic band for Fe_3O_4 at 570 cm^{-1} due to Fe–O stretching band [21] that confirms the presence of the magnetic core. The absorption peak at about 3400 cm^{-1} is originated by hydroxyls (OH), while bands at 2925 and 1396 cm^{-1} is most likely due to the stretching CH and CH_2 scissoring in humic acid. The coating of Fe_3O_4 by HA is confirmed by the presence of bands, at ~ 1620 cm^{-1} which is due to C=O stretching (Fig. 2c), indicating that the carboxylate anion interacts with the FeO surface [22].

The surface morphology of Fe_3O_4 and Fe_3O_4/HA was investigated by transmission electron microscope (TEM). The image of TEM was shown in Fig. 3a, b where most of the magnetite nanoparticles were found to be quasi-spherical, with a mean size of around 15 nm. The improvement in the dispersion may be due to that the HA weaken the interaction between the magnetite particles.

Sorption study

Effect of pH

In order to explain the sorption behavior and mechanism of the aqueous species of U(VI), the distribution species of U(VI) as a function of pH was calculated. The effect of pH was investigated in the range of 2.5–7.0 for Fe_3O_4 and in the range of 2.5–6.0, in the case of Fe_3O_4/HA. It is clear that the uptake increases with pH of the solution, Fig. 4. As the Fig. 4 shows, the sorption of U(VI) on Fe_3O_4 increases largely with increasing pH. In case of Fe_3O_4/HA, the behavior is different: at pH < 5 humic acid causes an increase of the U(VI) uptake into Fe_3O_4/HA (as compared with Fe_3O_4), while at pH > 5 the release of humic material from the associate into the solution and the formation of dissolved uranyl humate complexes cause a reduction of the U(VI) uptake. The relative distribution of aqueous U(VI) species in solution at a concentration of 2×10^{-4} mol/L is presented in Fig. 5, using Visual MINTEQ ver. 3.0.33 l [23]. It is clear that the soluble uranyl hydroxo complex $(UO_2)_3(OH)_5^+$ and $(UO_2)_4(OH)_7^+$ are the predominant species at pH range of 5.0–7.0, that favors the interaction between the functional groups that exist at the magnetite surface (=FeOOH), in addition to the presence of carboxylic and phenolic groups on humic acid [24].

Effect of contact time

The effect of contact time was studied at a time of 5.0–180.0 min., at 25 °C with initial concentration of

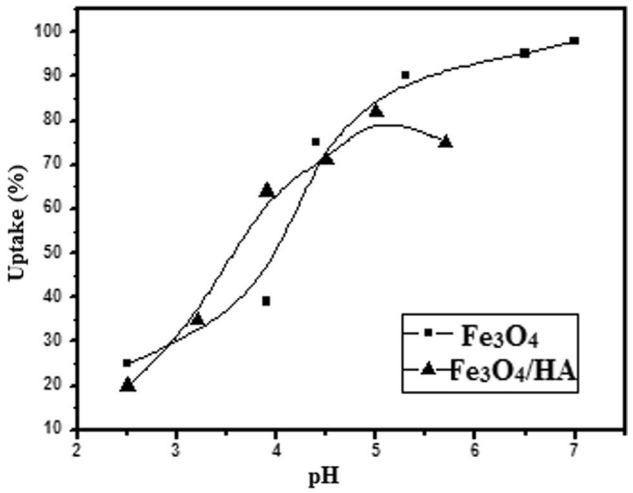

Fig. 4 Effect of pH on the sorption of UO_2^{2+} by Fe_3O_4 and Fe_3O_4/HA

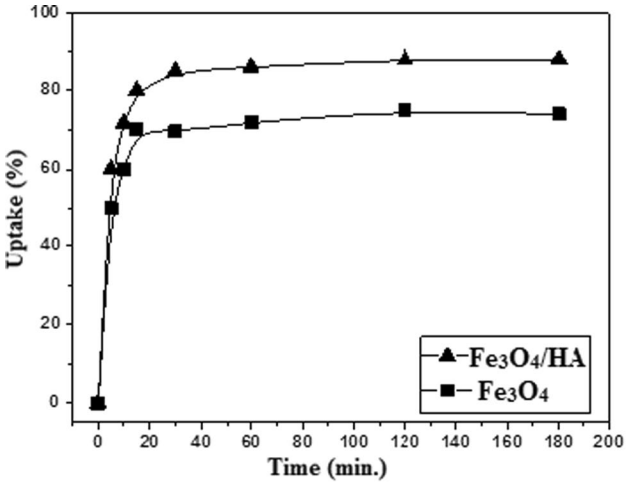

Fig. 6 Effect of contact time on the sorption of U(VI) ions by Fe_3O_4 and Fe_3O_4/HA

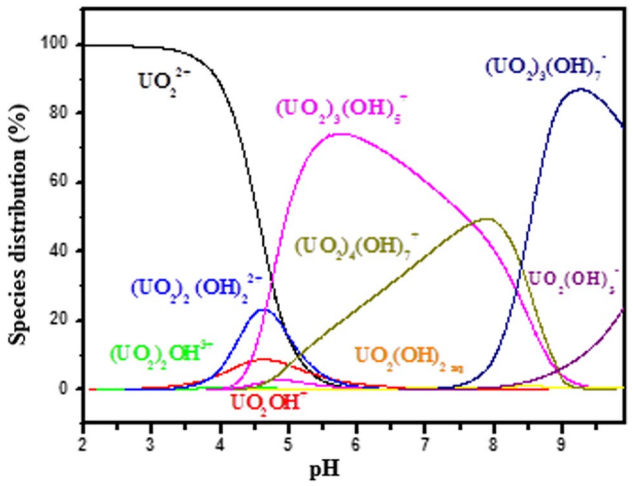

Fig. 5 Species distribution of uranyl ions

50 mg/L for uranium(VI), Fig. 6. The results show that the equilibrium was attained within 60 min, after that, the sorption remained nearly constant due to the saturation of the sorption sites on the surface of nanomagnetite, while the humic acid enhances the sorption due to the presence of phenolic and carboxylic groups in its structure.

Kinetic investigations were performed to elucidate the mechanism of adsorption of metal ions, explain how fast the rate of chemical reaction occurs and also to know the factors affecting the reaction rate. Among them; three kinetic models (the Lagergren's pseudo-first order kinetic model, pseudo-second order model and intraparticle diffusion models) were used for examination of our experimental data.

The pseudo-first-order equation was suggested by Lagergren, for the adsorption of solid–liquid systems. It is generally expressed as follows:

$$\log(q_e - q_t) = \log q_e - \left(\frac{k_1}{2.303}\right)t \tag{3}$$

The sorption data were also investigated by pseudo-second-order mechanism. In this model, the rate-limiting step is the surface adsorption that involves chemisorption [25]. The pseudo-second-order adsorption kinetic rate equation is expressed as:

$$\left(\frac{t}{q_t}\right) = \left(\frac{1}{k_2 q_e^2}\right) + \left(\frac{1}{q_e}\right) t \tag{4}$$

where q_e and q_t (mg/g) refer to the amount of metal ions adsorbed on both adsorbents at equilibrium and at time (t),

Table 1 Comparison of the pseudo first, second-order and intra-particle diffusion constants, calculated and experimental q_e values, for U(VI) ions onto Fe_3O_4 and Fe_3O_4/HA

Adsorbent	First-order kinetic parameters			Second-order kinetic parameters			Intra-particle diffusion			q_e, exp. (mg/g)
	k_1 (min^{-1})	q_e, calc. (mg/g)	R^2	k_2 (g/mg min)	q_e, calc. (mg/g)	R^2	k_i (mg g^{-1} $min^{-0.5}$)	C	R^2	
Fe_3O_4	0.038	65.0	0.85	1.5×10^{-3}	115.7	0.998	1.5	25	0.996	113.8
Fe_3O_4/HA	0.039	80.0	0.92	1.8×10^{-3}	125.0	0.999	1.2	107	0.994	121.0

respectively. k_1 is the rate constant of pseudo-first-order (min^{-1}), while k_2 (gmg^{-1} min^{-1}) is the rate constant of the second-order adsorption. The rate constants were calculated and tabulated in Table 1. As the calculated equilibrium sorption shows, the capacity (q_e) from the second-order kinetic model is consistent with the experimental data, Table 1. Therefore, the sorption can be described by pseudo-second-order kinetic model, Fig. 7a–c.

The intraparticle diffusion model is expressed as the following equation:

$$q_t = k_i t^{1/2} + C \tag{5}$$

where k_i (mg g^{-1} $min^{-0.5}$) is the intra-particle diffusion rate constant and C is the intercept which is proportional to the boundary layer thickness, Fig. 7c. The linear relationships that do not pass through the origin point that infers the intra-particle diffusion is not the dominant mechanism in processes occurring during the sorption of U(VI) ions on Fe_3O_4 and Fe_3O_4/HA. The other mechanisms such as film diffusion or particle diffusion may control the sorption process [26], and the parameters are listed in Table 1.

Effect of metal ion concentration

The effect of metal ion concentration on the sorption of U(VI), by Fe_3O_4 and Fe_3O_4/HA is studied in the range of 10–300 mg/L, at different temperatures and the results are indicated in Figs. 8a, b and 9a, b. Figure 8a, b indicates the effect of variation of the metal ion concentration on the sorption route. It is clear from the figures that, the percentage of uptake is gradually decreased by increasing the metal ion concentration. The seeming decrease in the uptake indicates that the metal ions included in the system, after reaching equilibrium, stay in solution. When a cation is accepted by a sorbent, a cation-exchange site is eliminated, dropping the effective cation-exchange capacity [27].

Plotting the amount of metal retained by the sorbent materials (as derived from Fig. 8a, b) against the metal ion concentration, gives the Fig. 9a, b.

It is clear from the figures that, as the concentration of U(VI) ions increases, their amount adsorbed (q) onto Fe_3O_4 and Fe_3O_4/HA increase till equilibrium attained at which a limited number of sites on the nanoparticle surfaces are available for the sorption. The presence of humic acid seems to retard the sorption of U(VI), this may be explained as: with increasing the concentration of U(VI), more U(VI) is available for complexation with humic acid where a soluble uranyl-humate complex is formed [28]. Thus, the competition between uranyl- humate complex formation and surface complexation arises and lead to a decrease in the sorption of U(VI) on magnetite coated humic acid.

Isotherm models

In this study, Langmuir and Freundlich isotherm models were tested to find the best fitting equations. In Langmuir isotherm model, the linear form is represented by the following equation:

$$\frac{C_e}{q_e} = \frac{1}{bQ^o} + \frac{1}{Q^o}C_e \tag{6}$$

where q_e is the amount adsorbed (mg/g), C_e is the equilibrium concentration of the metal ion (mg/L), and Q^o and b are Langmuir constants related to the adsorption capacity and binding energy between the adsorbent and the adsorbate, respectively. These constants can be calculated by plotting of C_e/q_e against C_e. The results are illustrated in Fig. 10a, b and Table 2.

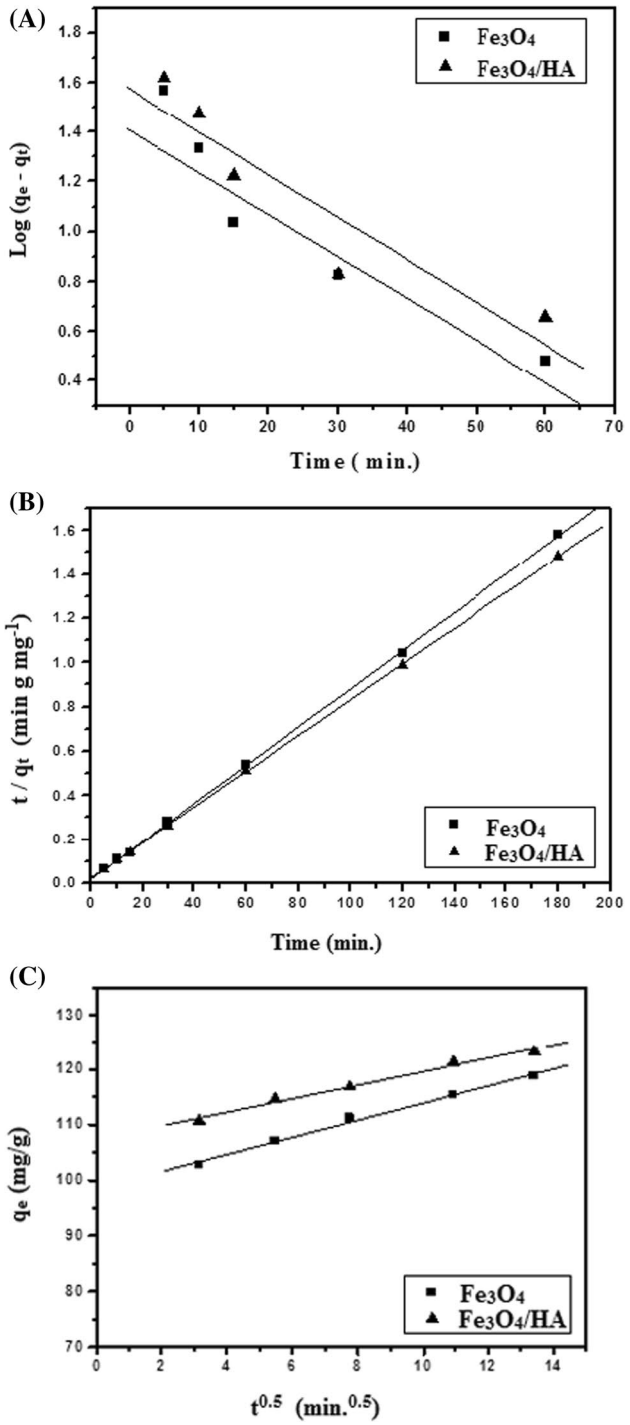

Fig. 7 **a** Pseudo- first order plot for the sorption of U(VI) on Fe_3O_4 and Fe_3O_4/HA. **b** Pseudo-second-order plot for the sorption of U(VI) on Fe_3O_4 and Fe_3O_4/HA. **c** Intra-particle diffusion for the sorption of U(VI) on Fe_3O_4 and Fe_3O_4/HA

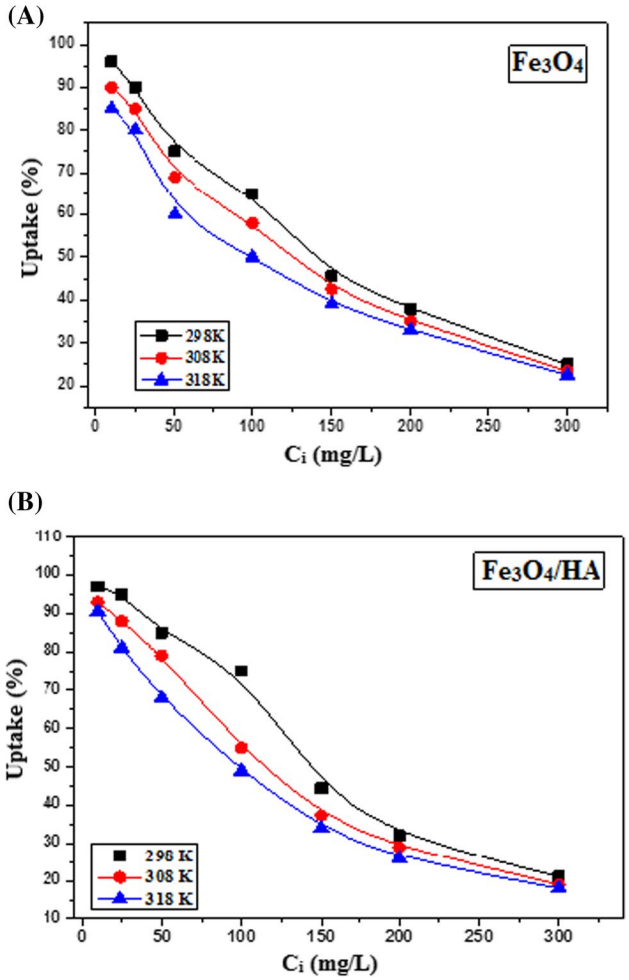

Fig. 8 **a** Variation of U(VI) concentration with the % uptake for Fe_3O_4 at different temperatures. **b** Variation of U(VI) concentration with the % uptake for Fe_3O_4/HA at different temperatures

The linear equation of Freundlich model is commonly represented as:

$$\log q_e = \log k_f + (1/n) \log C_e \quad (7)$$

where k_f and n are the Freundlich constants characteristics of the system, indicating the adsorption capacity and the adsorption intensity, respectively; that were estimated from the plot of log q_e versus log C_e, Fig. 11a, b and tabulated in Table 2. The regression correlation coefficient R^2 values for

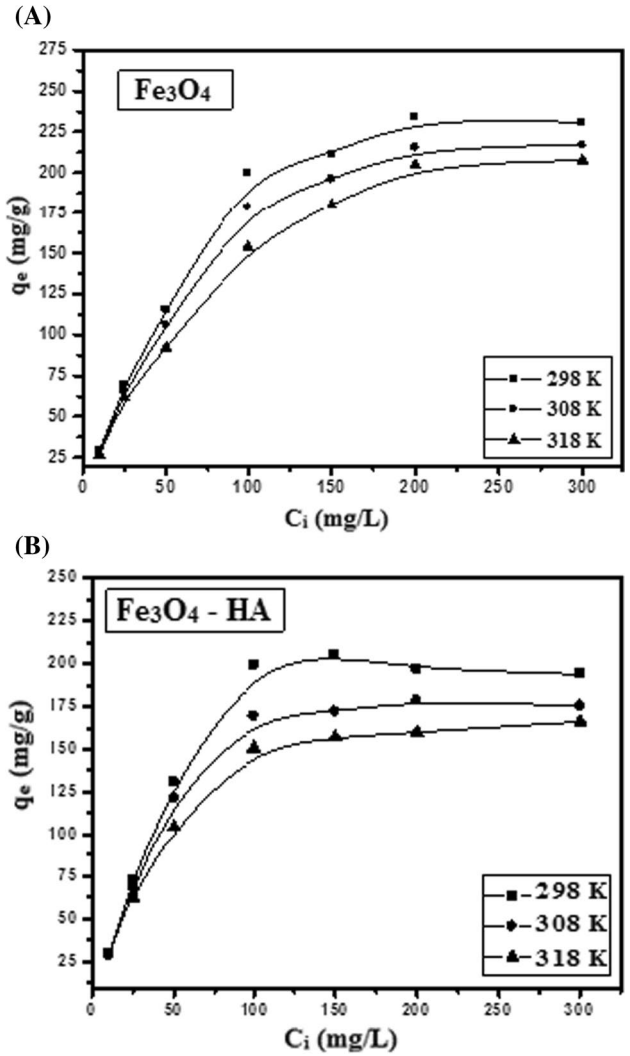

Fig. 9 **a** Variation of U(VI) concentration with the amount adsorbed for Fe_3O_4 at different temperatures. **b** Variation of U(VI) concentration with the amount adsorbed for Fe_3O_4/HA at different temperatures

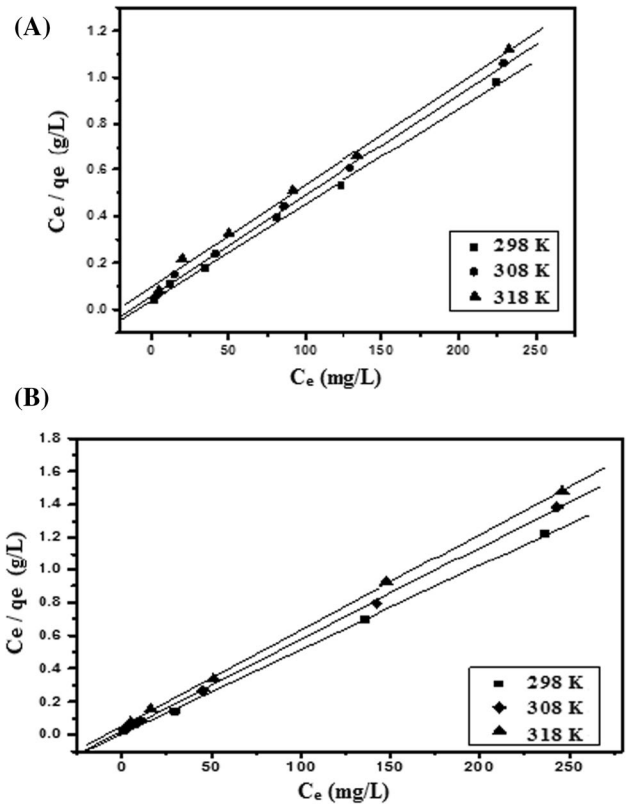

Fig. 10 **a** Langmuir plot for the sorption of U(VI) on Fe_3O_4 at different temperatures. **b** Langmuir plot for the sorption of U(VI) on Fe_3O_4/HA at different temperatures

Table 2 Langmuir and Freundlich parameters for the sorption of U(VI) on both Fe_3O_4 and Fe_3O_4/HA

Adsorbent	Langmuir parameters			Freundlich parameters		
	b (L/mg)	$Q^{O}_{max.}$ (mg/g)	R^2	n	K_f (mg/g)	R^2
Fe_3O_4	0.12	238	0.999	3.75	57	0.964
Fe_3O_4/HA	0.11	195.6	0.999	5.37	82	0.930

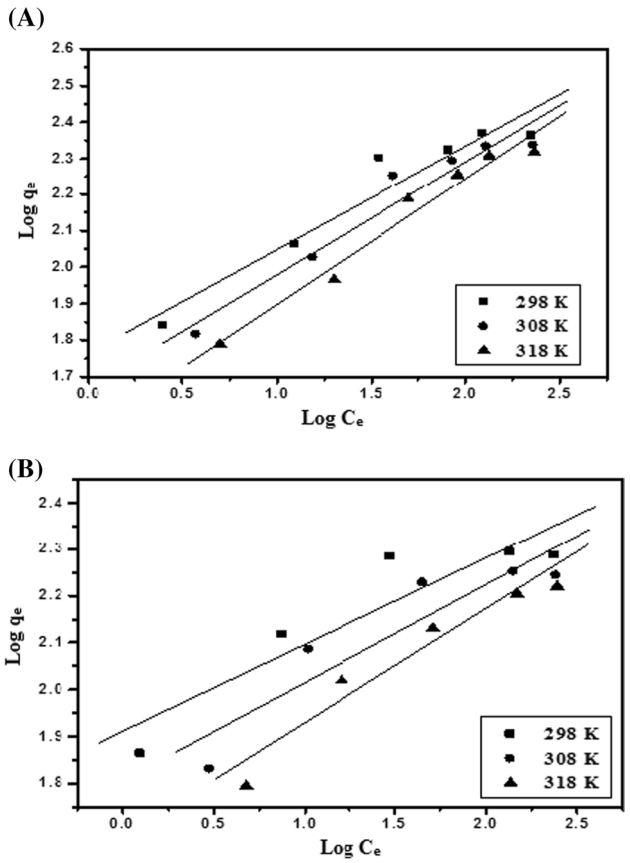

Fig. 11 **a** Freundlich plot for the sorption of U(VI) on Fe_3O_4 at different temperatures. **b** Freundlich plot for the sorption of U(VI) on Fe_3O_4/HA at different temperatures

the Langmuir equation in case of the two investigated adsorbents are higher than those obtained from the Freundlich equation implying that the adsorption isotherm data are well fitted by the Langmuir isotherm. The maximum adsorption capacity Q_{max} values were found to be 238.0, 195.6 mg/g for Fe_3O_4 and Fe_3O_4/HA, respectively; that are close to q_{exp}, Table 2. The capacity in case of Fe_3O_4/HA is lower since the presence of HA cause an occupation of some sorption sites.

A comparison of the adsorption performance of Fe_3O_4 and Fe_3O_4/HA with other adsorbents was reported in Table 3. The results implied that the investigated adsorbents can used efficiently for the uptake of U(VI) from aqueous medium.

Conclusion

A magnetite nanoparticle system and magnetite coated with humic acid were prepared, characterized, and applied to the removal of uranium ions. Fe_3O_4/HA has a maximum capacity of 195.6 mg/g, while Fe_3O_4 has a maximum capacity of 238.0 mg/g. Pseudo-second order and Langmuir isotherm models explain the sorption data. The presence of humic acid decreases the capacity as it causes a polyanionic organic coating and alters the particle surface properties. The results suggest that the magnetite nanoparticles can be used for the treatment of nuclear plants from radioactive uranium waste.

Table 3 Comparison of sorption capacities for U(VI) using various adsorbent materials

Sorbent	Q_{max}, mg/g	Optimum pH	References
Oxime-grafted mesoporous carbon	65.18	4.5	[29]
Chitin based marine sponges	288.0	7.0	[30]
Rice straw (AC)	100.0	5.5	[31]
Banyan leaves	22.06	3.0	[32]
Graphine oxide	97.5	5.0	[33]
Fe_3O_4-GO	69.49	5.5	[34]
Mesoporous MnO_2/SBA-15	465.1	6.0	[35]
MWCNTs	39.5	5.0	[36]
Silica coated -coated NPs Fe_3O_4	52.4	6.0	[17]
NANO magnetite	238.0	7.0	(This study)
NANO magnetite coated HA	195.6	5.0	(This study)

Acknowledgements The authors thank all the staff members and colleagues of the Hot Laboratories Centre and Nuclear Research Center of Egyptian Atomic Energy Authority for their cooperation, and useful help offered during this work.

Funding Open access funding provided by The Science, Technology & Innovation Funding Authority (STDF) in cooperation with The Egyptian Knowledge Bank (EKB).

References

1. WHO (2008) Guidelines for drinking-water quality: second addendum, vol 1, Recommendations
2. Chandra C, Fahmida K (2020) Nano-scale zerovalent copper: green synthesis, characterization and efficient removal of uranium. J Radioanal Nucl Chem 324:589–597. https://doi.org/10.1007/s10967-020-07080-1
3. Hossein F, Mohammad M, Alireza F, Mozhgan I (2014) Evaluation of a new magnetic zeolite composite for removal of Cs^{+} and Sr^{2+} from aqueous solutions: kinetic, equilibrium and thermodynamic studies. C R Chim 17(2):108–117. https://doi.org/10.1016/j.crci.2013.02.006
4. Wang S, Guo W, Gao F, Wang Y, Gao Y (2018) Lead and uranium sorptive removal from aqueous solution using magnetic and nonmagnetic fast pyrolysis rice husk biochars. RSC Adv 8:13205–13210. https://doi.org/10.1039/C7RA13540H
5. Pragnesh ND, Lakhan VC (2014) Application of iron oxide nanomaterials for the removal of heavy metals. J Nanotechnol 2014:1–14. https://doi.org/10.1155/2014/398569
6. Ngenefeme FJ, Namanga JE, Yufanyi DM, Ndinteh DT, Krause WMR (2013) A one pot green synthesis and characterisation of iron oxide-pectin hybrid nanocomposite. OJCM 3:30–37. https://doi.org/10.4236/ojcm.2013.32005
7. Grazhulene S, Zolotareva N, Redkin A, Shilkina N, Mitina A, Kolesnikova A (2018) Magnetic sorbent based on magnetite and modified carbon nanotubes for extraction of some toxic elements. Russ J Appl Chem 91:1849–1855. https://doi.org/10.1134/S1070427218110162
8. Helal A, Mazario E, Mayoral A, Decorse P, Losno R, Lion C, Hémadi M (2018) Highly efficient and selective extraction of uranium from aqueous solution using a magnetic device: succinyl-β-cyclodextrin-APTES@maghemite nanoparticles. Environ Sci Nano 5(1):158–168. https://doi.org/10.1039/c7en00902j
9. Peng L, Qin PF, Lei M, Zeng QR, Song HJ, Yang J, Shao J, Liao BH, Gu JD (2012) Modifying Fe_3O_4 nanoparticles with humic acid for removal of Rhodamine B in water. J Hazard Mater 209:193–198. https://doi.org/10.1016/j.jhazmat.2012.01.011
10. Rashid M, Sterbinsky GE, Pinilla MAG, Cai Y, O'Shea KE (2018) Kinetic and mechanistic evaluation of inorganic arsenic species adsorption onto humic acid grafted magnetite nanoparticles. J Phys Chem 122(25):13540–13547. https://doi.org/10.1021/acs.jpcc.7b12438
11. Singhal P, Pulhani V, Ali SM, Ningthoujam RS (2019) Sorption of different metal ions on magnetic nanoparticles and their effect on nanoparticles settlement. Environ Nanotechnol Monit Manag 11:100202. https://doi.org/10.1016/j.enmm.2018.100202
12. Yang ST, Zong PF, Ren XM, Wang Q, Wan XK (2012) Rapid and highly efficient preconcentration of Eu(III) by core–shell structured Fe_3O_4@Humic acid magnetic nanoparticles. ACS Appl Mater Interfaces 4(12):6890–6899. https://doi.org/10.1021/am3020372
13. Eilles E, Tombácz E (2003) The role of variable surface charge and surface complexation in the adsorption of humic acid on magnetite. Colloids Surf A Physicochem Eng Asp 230:99–109. https://doi.org/10.1016/j.colsurfa.2003.09.017
14. Sadeghi S, Azhdari H, Arabi H, Moghaddam AZ (2012) Surface modified magnetic Fe_3O_4 nanoparticles as a selective sorbent for solid phase extraction of uranyl ions from water samples. J Hazard Mater 215–216:208–216. https://doi.org/10.1016/j.jhazmat.2012.02.054
15. Zhao Y, Li J, Zhao L, Zhang S, Huang Y, Wu X, Wang X (2014) Synthesis of amidoxime functionalized Fe_3O_4 @SiO_2 core–shell magnetic microspheres for highly efficient sorption of U(VI). Chem Eng J 235:275–283. https://doi.org/10.1016/j.cej.2013.09.034
16. Tan L, Wang J, Liu Q, Sun Y, Zhang H, Wang Y, Jing X, Liu J, Song D (2015) Facile preparation of oxine functionalized magnetic Fe_3O_4 particles for enhanced uranium (VI) adsorption. Colloids Surf A Physicochem Eng Asp 466:85–91. https://doi.org/10.1016/j.colsurfa.2014.11.020
17. Fan FL, Qin Z, Bai J, Rong WD, Fan FY, Tian W, Wu XL, Wang Y, Zhao L (2012) Rapid removal of uranium from aqueous solutions using magnetic Fe_3O_4@SiO_2 composite particles. J Environ Radioact 106:40–46. https://doi.org/10.1016/j.jenvrad.2011.11.003
18. Singhal P, Jha SK, Pandey SP, Neogy S (2017) Rapid extraction of uranium from sea water using Fe_3O_4 and humic acid coated Fe_3O_4 nanoparticles. J Hazard Mater 335:152–161. https://doi.org/10.1016/j.jhazmat.2017.04.043
19. Marzenko Z (1986) Spectrophotometric determination of elements. Wiley, New York
20. Sun J, Zhou S, Hou P, Yang Y, Weng J, Li X, Li M (2007) Synthesis and characterization of biocompatible Fe_3O_4 nanoparticles. J Biomed Mater Res A 80A(2):333–341. https://doi.org/10.1002/jbm.a.30909
21. Carlos L, Cipollone M, Soria D, Moreno M, Ogillby P, Einschlag F, Martire D (2012) The effect of humic acid binding to magnetite nanoparticles on the photogeneration of reactive oxygen species. Sep Purif Technol 91:23–29. https://doi.org/10.1016/j.seppur.2011.08.028
22. Yantasee W, Warner C, Sangvanich T, Addleman R, Carter T, Wiacek R, Fryxell G, Timchalk CM, Warner M (2007) Removal of heavy metals from aqueous systems with thiol functionalized super paramagnetic nanoparticles. Environ Sci Technol 41:5114–5119. https://doi.org/10.1021/es0705238
23. Gustafsson JP (2012) Visual MINTEQ ver. 3.3. Department of Land and Water Resources Engineering, KTH (Royal Institute of Technology), SE-100 44, Stockholm, Sweden. Available at http://www2.lwr.kth.se/English/OurSoftware/vminteq/index.htm
24. Li D, Kaplan DI (2012) Literature review on the sorption of Plutonium, Uranium, Neptunium, Americium, and Technetium to Corrosion Products on Waste Tank Liners. SRNL-STI-2012-00040, Savannah River National Laboratory
25. Ahmed IM, Gamal R, Helal Aly A, Abo-El-Enein SA, Helal AA (2017) Kinetic sorption study of cerium(IV) on magnetite

nanoparticles. Part Sci Technol 35(6):643–652. https://doi.org/10.1080/02726351.2016.1192572
26. Jaeshik C, Jinyoung C, Jinwoo L, Sang HL, Young JL, Seok WH (2012) Sorption of Pb(II) and Cu(II) onto multi-amine grafted mesoporous silica embedded with nano-magnetite: effects of steric factors. J Hazard Mater 239:183–191. https://doi.org/10.1016/j.jhazmat.2012.08.063
27. Helal AA, Helal Aly A, Salim NZ, Khalifa SM (2006) Sorption of radionuclides on peat humin. J Radioanal Nucl Chem 267(2):363–368. https://doi.org/10.1007/s10967-006-0056-2
28. Saches S, Brendler G, Geipel G (2007) Uranium(VI) complexation by humic acid under neutral pH conditions studied by laser-induced fluorescence spectroscopy. Radiochim Acta 95:103–108. https://doi.org/10.1524/ract.2007.95.2.103
29. Tian G, Geng J, Jin Y, Wang C, Li S, Chen Z, Wang H, Zhao Y, Li S (2011) Sorption of uranium(VI) using oxime-grafted ordered mesoporous carbon CMK-5. J Hazard Mater 190:422–450. https://doi.org/10.1016/j.jhazmat.2011.03.066
30. Schleuter D, Silvia A, Zoran H, Hanke T, Bernhard G, Brunner E (2013) Chitin based renewable materials from marine sponges for uranium adsorption. Carbohydr Polym 92:712–720. https://doi.org/10.1016/j.carbpol.2012.08.090
31. Yakout S, Metwally S, El-Zakla T (2013) Uranium sorption onto activated carbon prepared from rice straw: competition with humic acids. Appl Surf Sci 280:745–750. https://doi.org/10.1016/j.apsusc.2013.05.055
32. Xia L, Tan K, Wang X, Zheng W (2013) Uranium removal from aqueous solution by banyan leaves: equilibrium, thermodynamic, kinetic, and mechanism studies. J Environ Eng 139:887–894. https://doi.org/10.1061/(ASCE)EE.1943-7870.0000695
33. Zhao G, Wen T, Yang X, Yang S, Liao J, Shao D, Wang X (2012) Preconcentration of U(VI) ions on few-layered graphene oxide nanosheets from aqueous solutions. Dalton Trans 41:6182–6188. https://doi.org/10.1039/C2DT00054G
34. Zong P, Wang S, Zhao Y, Wang H, Pan H, He C (2013) RETRACTED: high sorption of U(VI) on graphene oxides studied by batch experimental and theoretical calculation. Chem Eng J 220:45–52. https://doi.org/10.1016/j.cej.2015.11.066
35. Ding Y, Xian Q, Wang E, He X, Jiang Z, Dan H, Zhu W (2020) Mesoporous MnO_2/SBA-15 as a synergetic adsorbent for enhanced uranium adsorption. New J Chem 44:13707–13715. https://doi.org/10.1039/D0NJ02966A
36. Fasfous I, Dawoud J (2012) Uranium(VI) sorption by multiwalled carbon nanotubes from aqueous solution. Appl Surf Sci 259:433–440. https://doi.org/10.1016/j.apsusc.2012.07.062